Fjord insertion into continental margins driven by topographic steering of ice

MARK A. KESSLER[1]*, ROBERT S. ANDERSON[1,2] AND JASON P. BRINER[3]

[1]Institute of Arctic and Alpine Research, University of Colorado, Boulder, Colorado 80309, USA
[2]Department of Geological Sciences, University of Colorado, Boulder, Colorado 80309, USA
[3]Department of Geology, University at Buffalo, Buffalo, New York 14260, USA
*e-mail: mark.kessler@colorado.edu

Published online: 11 May 2008; doi:10.1038/ngeo201

Fjords commonly punctuate continental edges formerly occupied by Quaternary ice sheets, reaching kilometre depths and extending many tens of kilometres inland[1,2]. These features must have been created by late Cenozoic ice sheets, because rivers cannot erode bedrock much below sea level. Ice sheets drain primarily through fjords[3,4]; therefore, widespread fjord insertion may have altered ice-sheet size, shape and dynamics. Here, we use a two-dimensional ice-sheet model to simulate the incision of fjords through a coastal mountain range. We show that topographic steering of ice and erosion proportional to ice discharge are sufficient to form fjords. Within one million years, kilometre-deep fjords punched through the mountain range owing to a robust positive feedback initiated by ice being steered towards mountain passes. Enhanced erosion beneath thicker, faster ice deepens these passes, amplifying the topographic steering. Simulated fjords are deepest through the highest topography and drain a large fraction of the interior ice. Ice sheets simulated on landscapes with existing fjords are generally smaller and exhibit longer response times and larger responses to climate changes, suggesting that modern ice sheets are more sensitive to climate fluctuations than Early Quaternary ice sheets.

The introduction of fjords probably enabled strong co-evolution of landscape and glacial dynamics through the late Cenozoic era[5,6]. Recent thermochronologic studies in British Columbia suggest rapid fjord incision soon after the onset of Northern Hemisphere glaciation[7]. Cosmogenic radionuclide studies reveal sharp spatial gradients in erosion rates, with rates in fjords four orders of magnitude higher than on interfjord uplands[8–10]. This illustrates the strong control exerted by fjorded topography on spatial variations in erosion[11], probably reflecting in part the thermal state of the bed. This correlation between topography and bed thermal state would have been much weaker early in fjord development when topographic differences were small.

Although conceptual models of fjord formation exist[12–14], the feedback mechanisms responsible for fjords have not been modelled. Whereas numerical models of glacier erosion have shown small-scale topographic steering and suggest that ice convergence can cause valley overdeepening[15–18], fjord formation has not been investigated. In these models, erosion depends on an intermediate-timescale average basal sliding and subglacial hydrology. Acknowledging our poor knowledge of how to model subglacial hydrology and sliding averaged over timescales from hours to millennia, we eliminate the detailed physics of glacier sliding and erosion in an attempt to isolate the feedbacks and properties of the ice-sheet–landscape system that cause fjord incision.

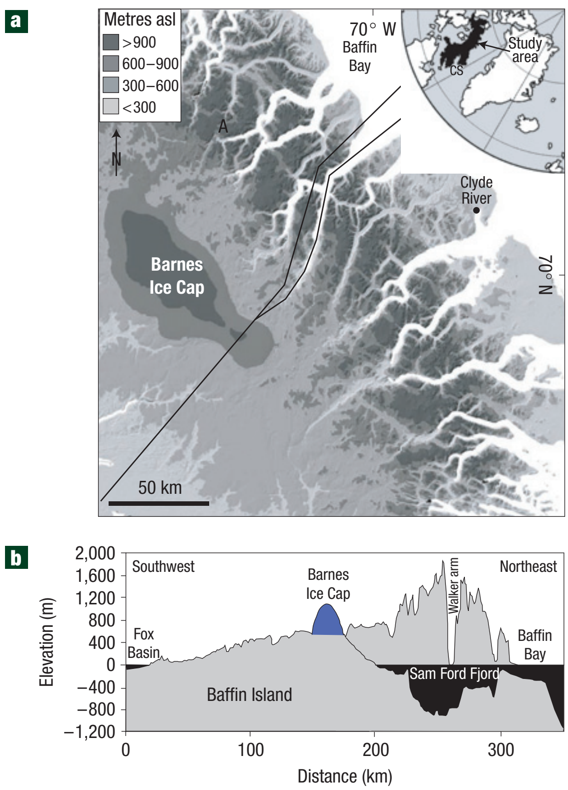

Figure 1 Baffin Island fjorded topography. a, The fjorded continental edge of northeastern Baffin Island showing the inland plateau, on which the Barnes Ice Cap sits, and the fringing mountain range (asl: above sea level). Inset: Location of Baffin Island in the western Arctic. **b**, Topographic cross-section of Baffin Island, along Sam Ford Fjord and neighbouring topography, following the transect lines shown in the map.

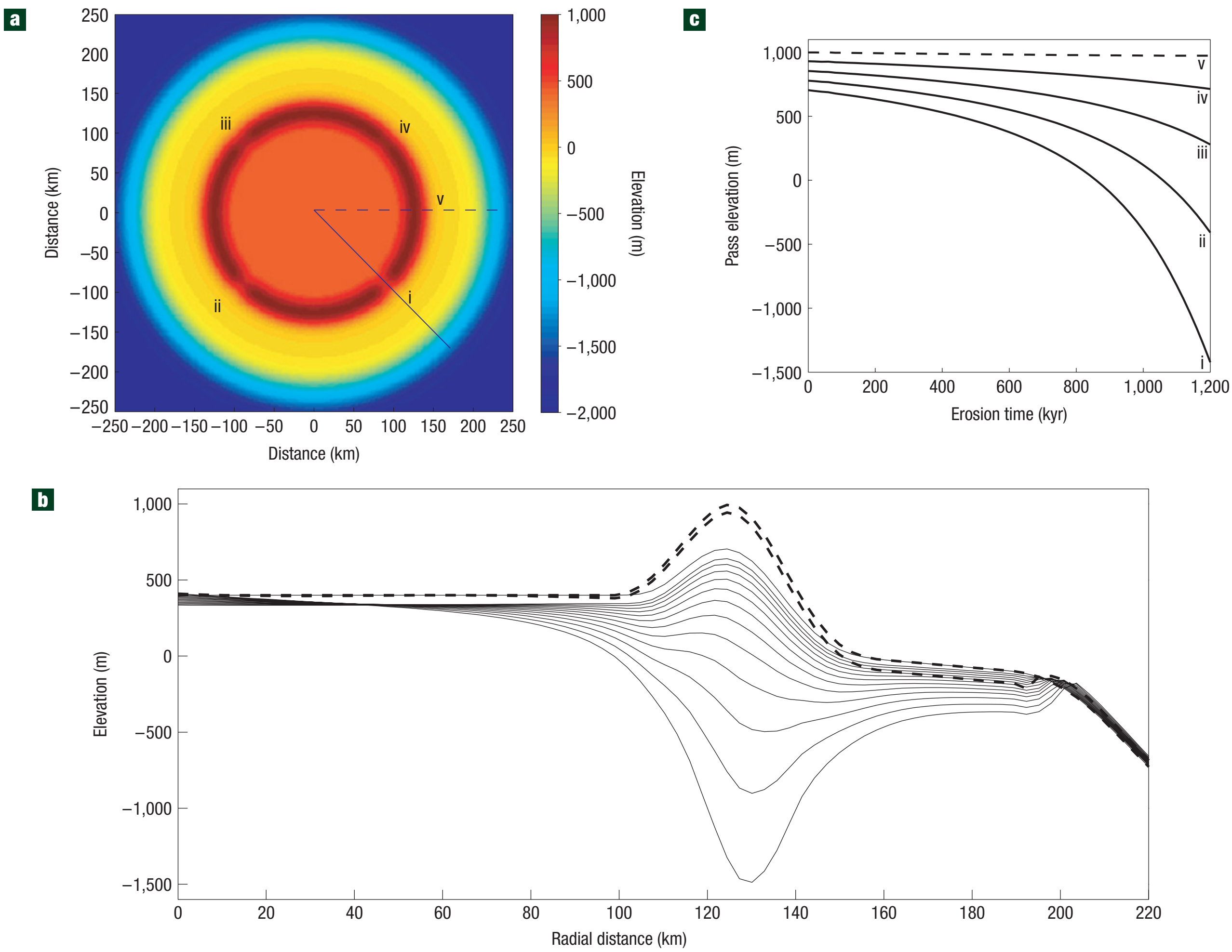

Figure 2 Evolution of model topography. a, Initial bed topography; a 50-km-wide, 1,000-m-high annular coastal mountain range surrounding a 200-km-wide, 400-m-high basin is dissected by four ∼20-km-wide (at half height) valleys with depths of 300, 225, 150 and 75 m below the ridge. **b**, Fjord evolution; thin solid lines indicate bed profiles at 100 kyr intervals for the deepest valley (transect 'i' in **a**); dashed bold lines indicate initial and final topographic profiles between valleys (transect 'v' in **a**). **c**, Elevation through time at the radial position of the initial crest for the four passes (i, ii, iii, iv) and the crest (v).

It has long been recognized that the production of such pronounced kilometre-scale relief from initially non-glacial continental margins requires a strong positive feedback between topography, ice flow and erosion rates[14,19]. The ubiquity of fjords on formerly glaciated coasts, such as Baffin Island (Fig. 1), Norway and Chile, indicates that this fjord feedback does not rely on the details of the coastal geometry, local climate or geology. We hypothesize that fjord creation requires only two properties of the ice-sheet–landscape interaction. First, as with any dense fluid, ice converges towards depressions in the underlying topography. Second, over long timescales, the pattern of ice discharge sets the pattern of erosion. This assumption that erosion increases with ice discharge, as data in Hallet *et al.*[20] imply, is an extreme simplification of the complex interactions between time-varying climates, ice sheets and their beds. However, this assumption acknowledges that processes that enhance ice discharge typically also increase the erosion rate[16,20], largely because basal sliding and erosion are driven by the same variables that govern ice discharge: ice thickness, slope and basal temperature.

The essence of topographic ice steering exists even in the basic equation of ice motion used in most first-order ice-sheet models: the vertically averaged ice speed ($\bar{U}$) due to shear deformation of isothermal ice is taken to be

$$\bar{U} = \frac{2A}{n+2}\left[\rho_i g S\right]^n H^{n+1}, \qquad (1)$$

in which A is Glen's flow law coefficient, ρ_i is ice density, g is gravity, S is ice surface slope, H is ice thickness and n is usually taken to be 3 (ref. 21). The strength of the positive feedback results from both the sensitivity of ice velocity to ice surface slope ($\propto S^n$), allowing for substantial steering and thickening of ice in valleys and passes, and the strong dependence of ice discharge ($q = \bar{U}H$), and hence erosion, on ice thickness ($\propto H^{n+2}$).

We use a rudimentary two-dimensional (plan view) glacial model[22] with ice motion given by equation (1) and bed erosion proportional to the ice discharge per unit width to test whether a fjord formation feedback exists in a first-order ice-sheet model and whether it can produce kilometre-scale fjord relief on a million-year timescale assuming realistic spatially averaged erosion rates ($0.1\ \mathrm{mm\,yr^{-1}}$)[20]. We target the Baffin Island coastline, located along the northeastern margin of the Laurentide ice sheet, with

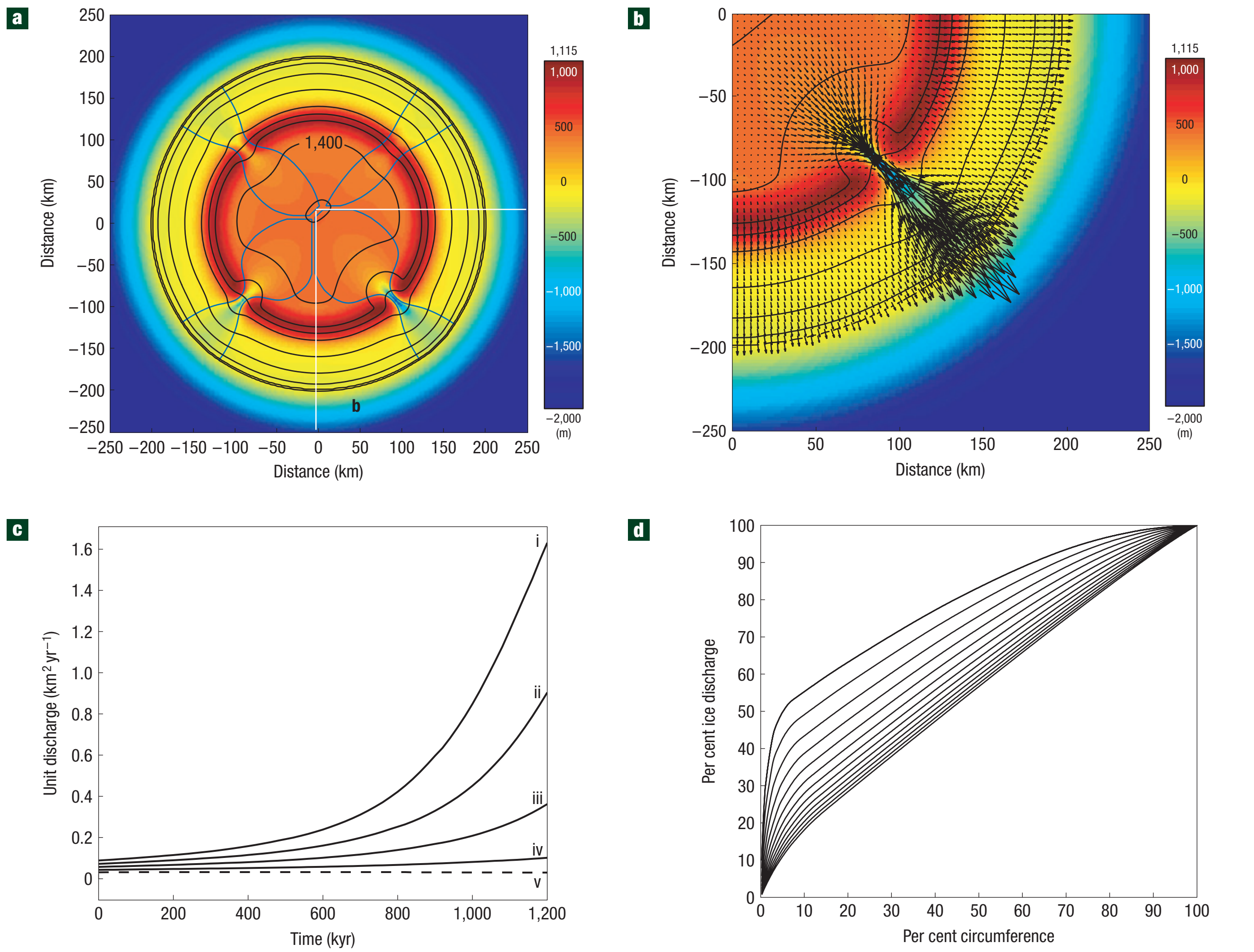

Figure 3 Modelled bed and ice flow after 1.2 Myr and ice discharge evolution. a, Bed elevation in false colour. Black lines denote 200 m ice surface contours. Blue lines demark regions that drain through each of the four valleys. **b**, Ice velocity vectors in the quadrant of the deepest valley. **c**, Specific ice discharge versus time through the four passes (i, ii, iii, iv) and over the crest (v) in Fig. 2a. **d**, Percentage of total ice discharge along the crest (125 km from centre) versus percentage of crest length through which that discharge passes, shown at 100 kyr intervals.

a ~1.5-km-high bounding mountain range 30–60 km inland from the coast (Fig. 1); this topography is characteristic of many fjorded coastlines, including Greenland, British Columbia and the Transantarctic Mountains. From their inland heads, Baffin fjords typically deepen in steps, are deepest (up to 900 m below sea level) as they cross the core of the bounding range, shallow towards their mouths, then transition into few-hundred-metre-deep troughs across the continental shelf (Fig. 1).

Well-developed fjords appear in our simulations after about one million years. Within 600 kyr, erosion defeats the lowest mountain pass, lowering it 300 m to the elevation of the interior basin (Fig. 2b,c). At this point, pre-glacial drainages inland from fringing mountain ranges would begin to reverse, emptying instead into the ocean. Accelerating erosion (Fig. 2c) lowers the resulting trough a further 1,900 m by 1.2 Myr, reaching 1,500 m depth. Over the same interval, the range crest lowers an average of 5 m (Fig. 2b). These results are consistent with other studies[7] that reveal rapid production of glacial troughs. These erosion times are linearly proportional to the erosion constant that we have chosen to yield spatial average erosion rates of ~0.1 mm yr^{-1} (ref. 20), resulting in erosion rates of <0.1 mm yr^{-1} over most of the simulation space, >0.2 mm yr^{-1} in fjord onset zones and low passes and up to 10 mm yr^{-1} in 1.5-km-deep fjords. Our model suggests that it is the increasingly non-uniform distribution of erosion resulting from the topography–ice flow–erosion feedback that enables rapid fjord incision; in contrast, 1–3 million years of erosion at 0.1 mm yr^{-1} would only lower mountain passes 300 m. Because the fjord feedback results from general properties of ice-sheet–landscape interactions, we expect that this same mechanism is responsible for earlier Cenozoic fjord formation on Antarctica and that other models of this system[15,17,18] will produce fjords if run with similar timescales, length scales and topographies. Our use of a low average erosion rate (0.1 mm yr^{-1}) both acknowledges that the landscape is not always glaciated and serves as a stronger test of the fjord formation mechanism.

The details of simulated fjords also mimic natural fjords. The deepest fjord ('i' in Fig. 2a) is >100 km long, having incised >30 km inland of the range crest. The depth profile exhibits a maximum near the range crest, matching well the geometry of fjords on Baffin Island[23] (Fig. 1). Beyond the constriction, ice flow

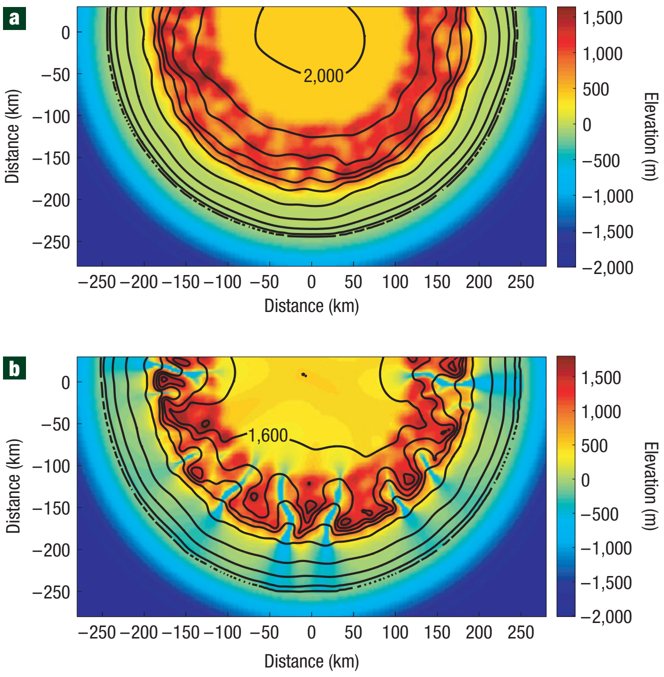

Figure 4 Modelled topographic and ice surface evolution with a randomly crenulated coastal mountain range. a,**b**, Initial (**a**) and after 1.2 Myr (**b**) states of a simulation using a random initial range topography generated by adding white noise to a two-peak sinusoidal range, followed by heavy smoothing. The bed is in false colour and the ice surface is contoured (200 m contours). The central 50 km annulus of the 100-km-wide random range has mean elevation of 990 m, with typical peak-to-valley amplitudes of ~500 m and typical wavelengths between 30 and 50 km.

diverges (Fig. 3a,b), producing a pattern of decreasing discharge per unit width and hence decreasing erosion, resulting in a fjord that shallows seaward of the bounding mountain range (Fig. 2b).

Increasing relief enhances lateral steering of ice and increases the area contributing ice to fjords (Fig. 3a). After 1.2 Myr, the deepest fjord drains ~3.5 times the area drained by the shallowest fjord ('i' and 'iv' respectively in Fig. 2a). The wrinkled ice surface reflects topographic steering well upstream of the range crest: ice surface concavity causes ice flow that strongly converges towards deep fjords (Fig. 3a,b). This produces a fjord that shallows smoothly upstream into a broadening onset zone that extends 40–60 km inland (Fig. 2a,b). The progressive capture of ice contributing area is also reflected in the nonlinear, 16-fold, increase in maximum ice discharge in the deepest fjord over 1.2 Myr (Fig. 3c). Whereas the four valleys (5% of the model circumference) initially carry 10% of the total ice discharge, they deliver 50% of the total ice discharge by 1.2 Myr (Fig. 3d); the deepest fjord carries 75% of the total ice discharge from its quadrant. This mimics Devon Icecap, where several tens of per cent of the ice drains through 4% of its margin[4].

In an extra simulation (Fig. 4), we use random mountain range topography to test whether rapid fjord development is a modelling artefact of ice funnelling through distinct passes on an otherwise uniform crest. Fjords again exploit low passes in the initial topography and erode the ridges between them to form continuous paths from the interior basin out to the edge of the continental shelf.

We explored model sensitivity with a suite of simulations measuring the formation time of 1-km-deep fjords. Because of its control on topographic steering, doubling the relief above the deepest valley reduces formation time by 52%; eliminating the mountain range altogether, leaving an incised plateau, triples to quadruples the formation time. The total ice flux matters as well: doubling either the interior diameter or the net mass balance reduces the formation time by 32%. Simulations with 8 or 16 equal-depth valleys take 14% and 39% longer to form 1-km-deep fjords than simulations with 4 or fewer equal-depth valleys. Although mass balance, interior diameter, mountain range relief and the number of valleys influence formation time, none prevents Quaternary timescale fjord incision.

In a final simulation, we initiated an ice sheet on topography with four mature 1-km-deep fjords. Using the same climate as in the original simulation, the steady-state ice volume is 35% smaller than on the initial non-fjorded topography, consistent with suggestions that fjords limit ice-sheet extent for a given climate[5,24]. In addition, the ice sheet on fjorded topography is much more sensitive to climate swings; it shrinks in volume by 9.4% with a 300 m rise in equilibrium line altitude compared with only 1.5% in the non-fjorded case. This is consistent with other work suggesting that low-gradient calving outlet glaciers that ring present ice sheets are sensitive to climate change[24] and can react to warming by catastrophic retreat[25,26]. The presence of fjords also lengthens the intrinsic timescale for ice-sheet growth (432 yr versus 210 yr; timescale over which the distance from steady-state ice volume decreases by 1/e), measured by exponential asymptotic growth of ice volume towards steady state; with fjords, the ice sheet takes twice as long to reach steady state.

To expose the fundamental feedback of fjord incision, we have omitted several important features of ice sheets: subglacial hydrology, ice sliding and most importantly the basal thermal regime. We argue that our model is conservative because these features all serve to enhance the fundamental fjord incision mechanism captured in our model. Thermal variation and basal sliding, for example, promote relief generation because thicker ice is warmer, has lower average viscosity and is more likely to slide, thus promoting higher erosion rates in topographic lows. By omitting the climate history that drives repeated advance and retreat of ice sheets, our model overestimates the long-term erosion rate for a given erosion constant, but underestimates relief production because in nature ice sheets occupy valleys before overriding a bounding range crest and therefore valleys erode for a greater fraction of the glacial cycle. Some processes ought to reduce fjord incision rate; for example, interglacial sediment fill takes longer to evacuate as fjords deepen, thus reducing the time available to erode bedrock. This limits the maximum depth of fjords by providing a negative feedback on fjord deepening.

Insertion of fjords carries several consequences. The newly created low-gradient calving outlets for interior ice probably enhanced ice-sheet sensitivity to climate and increased their degree of coupling with ocean dynamics. Because fjords efficiently drain ice-sheet interiors, building and maintaining large ice sheets presumably became more difficult through time as these topographic leaks became more efficient[5,24], as our modelling shows. If a critical ice-sheet size is required to trip a glacial–interglacial transition, widespread fjord insertion would have made this more difficult, perhaps contributing to the Middle Quaternary change in glacial interval from 40 kyr to 100 kyr. Entirely new ice-sheet dynamics are introduced, such as the catastrophic retreat of outlet glaciers occupying fjords[25,26], which provides a potential trigger for abrupt climate change[27] that may not have existed in the Early Quaternary. Fjord insertion can reverse pre-existing fluvial drainages. Finally, that a robust fjord feedback requires only two general properties of the ice-sheet–landscape system has enabled widespread insertion of deep, long fjords into edges of polar land masses over the course of the Quaternary.

METHODS

We used the two-dimensional (plan view), depth-averaged, isothermal, glacier model implemented in ref. 22, modified to include iceberg calving proportional to water depth[21], point load flexural isostatic compensation[6] and bed erosion proportional to the ice discharge per unit width (specific discharge). Ice motion was limited to internal deformation (equation (1)). This finite-difference code simulates ice moving over an underlying topography on a regular grid by solving the mass continuity equation for the rate of change in ice thickness ($\mathrm{d}H/\mathrm{d}t$) in each cell given the depth-averaged ice velocity ($\bar{U}$) specified by equation (1) and climate specified by the net mass balance (b_z):

$$\frac{\mathrm{d}H}{\mathrm{d}t} = b_z - \frac{\mathrm{d}q_x}{\mathrm{d}x} - \frac{\mathrm{d}q_y}{\mathrm{d}y}$$

$$q = \bar{U}H,$$

in which q is the specific ice discharge[16,21,28]. The ice thicknesses are stepped forward in time through multiplication of $\mathrm{d}H/\mathrm{d}t$ by a finite time interval Δt ($\sim$0.1 yr). The net mass balance as a function of elevation was chosen to coincide with estimates of climate during glaciation[29], and is specified by a 0.5 m km^{-1} linear increase with surface elevation from zero at 300 m (the equilibrium line altitude) up to a maximum of 0.5 m yr^{-1}.

Iceberg calving is simulated after each time step as a discrete process that removes ice from cells at the ice margin that have bed elevations below sea level. The ice volume removed generates a retreat rate of the ice margin that is linearly proportional to the water depth (ref. 21): $u_c = ch_\mathrm{w}$, in which c is an empirical constant and h_w is the water depth. In these simulations, sea level was chosen to put the calving front near the edge of the continental shelf during full glaciation ($\sim$80 m below the isostatically compensated coast) to minimize the impact of calving on the fundamental fjord feedback mechanism. As with our other assumptions, we are being conservative in assessing the fjord feedback: simulations run with higher sea level, in which greater calving leads to greater ice discharge, develop fjords more rapidly.

Isostatic compensation due to both ice loading and erosional unloading was implemented through a standard point load deflection of the lithosphere assuming an effective elastic thickness of 20 km (ref. 6). As the flexural calculation is computationally expensive, and the response time dictated by mantle viscosity is of the order of 1,000 yrs, we carry out the flexural isostatic calculation only every 100 simulation years.

Before each simulation, the model is spun-up by simulating the ice dynamics and isostatic compensation described above until the ice-sheet geometry is in steady state with the mass balance. Our initial topography (Fig. 2a) is an annular coastal mountain range containing fluvial valleys that control the location of fjords as observations suggest[30]. Thus, the initial condition for the landscape erosion simulation is a coastal mountain range overridden by a steady-state ice sheet in which calving and net ablation of ice at low elevations balances net accumulation at high elevations. Simulations were run on 250 × 250 cell square grids with a cell size of 2 km; simulations with 1 and 4 km grid cells differed only slightly from the results presented here.

Erosion is simulated at each time step. Bed elevation is lowered in proportion to the local ice discharge per unit width, q:

$$\Delta Z_\mathrm{b} = -\alpha q f \Delta t, \tag{2}$$

in which α is an erosion constant ($\alpha = 5 \times 10^{-9}$ m^{-1}) and f(= 200) is a scaling factor that accelerates erosion. As substantial bed erosion occurs on the 100 kyr timescale, whereas ice responds on a 100–1,000 yr timescale, large erosional steps can be used while maintaining the ice-sheet geometry near steady state with the steady climate forcing. The erosion factor, f, enables us to simulate 2 Myr of bed erosion while simulating only 10,000 yrs of ice dynamics. The erosion constant, α, was chosen to produce a conservative long-term average erosion rate across the glaciated area of $\sim$0.1 mm yr^{-1}. Transport and re-deposition of eroded sediment is not modelled; we assume that sediment is transported out of the system on timescales that are much shorter than the landscape erosion timescale.

We found that a negative feedback on fjord deepening is necessary in the random range simulation (Fig. 4) to enable fjord penetration through the wider range while maintaining maximum depths consistent with observed fjord depths around the world. We tapered the bed erosion (ΔZ_b) to zero by adding a weighting factor w to equation (2):

$$\Delta Z_\mathrm{b} = w(-\alpha q f \Delta t)$$

$$w = 1 - \left(\frac{|\min(0, Z_\mathrm{b})|}{L}\right)^m,$$

in which Z_b is the bed elevation and L(= 1 km) is an imposed maximum fjord depth. We used $m = 2$, reflecting the nonlinearly increasing strength of the negative feedbacks with fjord depth. The negative feedbacks that this is meant to mimic include the increasing fraction of a glacial period spent evacuating interglacial fjord sediment, which thickens as fjords deepen, and the decreasing fraction of the glacial period during which outlet glaciers are thick enough to be grounded and hence eroding through the fjords.

Received 7 January 2008; accepted 15 April 2008; published 11 May 2008.

References

1. Johnson, D. W. The nature and origin of fjords. *Science* **41**, 537–543 (1915).
2. Syvitski, J. P. M., Burrell, D. C. & Skei, J. M. *Fjords: Processes and Products* (Springer, New York, 1987).
3. Bennett, M. R. Ice streams as the arteries of an ice sheet: Their mechanics, stability and significance. *Earth Sci. Rev.* **61**, 309–339 (2003).
4. Dowdeswell, J. A., Benham, T. J., Gorman, M. R., Burgess, D. & Sharp, M. J. Form and flow of the Devon Island Ice Cap, Canadian Arctic. *J. Geophys. Res.* **109**, F02002 (2004).
5. Taylor, J. *et al*. Topographic controls on post-Oligocene changes in ice-sheet dynamics, Prydz Bay region, East Antarctica. *Geology* **32**, 197–200 (2004).
6. Stern, T. A., Baxter, A. K. & Barrett, P. J. Isostatic rebound due to glacial erosion within the Transantarctic Mountains. *Geology* **33**, 221–224 (2005).
7. Shuster, D. L., Ehlers, T. A., Rusmore, M. E. & Farley, K. A. Rapid glacial erosion at 1.8 Ma revealed by ^{4}He/^{3}He thermochronometry. *Science* **310**, 1668–1670 (2005).
8. Stroeven, A. P., Fabel, D., Harbor, J., Hättestrand, C. & Kleman, J. Quantifying the erosional impact of the Fennoscandian ice sheet in the Tornetrask-Narvik corridor, northern Sweden, based on cosmogenic radionuclide data. *Geograf. Ann. A* **84A**, 275–287 (2002).
9. Staiger, J. K. W. *et al*. Quaternary relief generation by polythermal glacier ice. *Earth Surf. Process. Landforms* **30**, 1145–1159 (2005).
10. Briner, J. P., Miller, G. H., Davis, P. T. & Finkel, R. C. Cosmogenic radionuclides from differentially weathered fiord landscapes support differential erosion by overriding ice sheets. *Geol. Soc. Am. Bull.* **118**, 406–420 (2006).
11. Nesje, A., Dahl, S. O., Valen, V. & Ovstedal, J. Quaternary erosion in the Sognefjord drainage basin, western Norway. *Geomorphology* **5**, 511–520 (1992).
12. Dury, G. H. A glacial breach in the northwestern highlands. *Scott. Geogr. Mag.* **69**, 106–117 (1953).
13. Holtedahl, H. Notes on the formation of fjords and fjord valleys. *Geograf. Ann. A* **49A**, 188–203 (1967).
14. Sugden, D. E. Glacial erosion by the Laurentide Ice Sheet. *J. Glaciol.* **83**, 367–391 (1978).
15. Braun, J., Zwartz, D. & Tomkin, J. A new surface-process model combining glacial and fluvial erosion. *Ann. Glaciol.* **28**, 282–290 (1998).
16. MacGregor, K. C., Anderson, R. S., Anderson, S. P. & Waddington, E. D. Numerical simulations of glacial-valley longitudinal profile evolution. *Geology* **28**, 1031–1034 (2000).
17. Herman, F. & Braun, J. Evolution of the glacial landscape of the Southern Alps of New Zealand: Insights from a glacial erosion model. *J. Geophys. Res.* (in the press).
18. Jamieson, S., Hulton, N. R. J. & Hagdorn, M. Modelling landscape evolution under ice sheets. *Geomorphology* **97**, 91–108 (2008).
19. Brown, R. Remarks on the formation of fjords and canons. *J. R. Geogr. Soc. Lond.* **41**, 348–360 (1871).
20. Hallet, B., Hunter, L. & Bogen, J. Rates of erosion and sediment evacuation by glaciers: A review of field data and their implications. *Glob. Planet. Change* **12**, 213–235 (1996).
21. Paterson, W. S. B. *The Physics of Glaciers* 3rd edn (Elsevier, New York, 1999).
22. Kessler, M. A., Anderson, R. S. & Stock, G. S. Modeling topographic and climatic control of east-west asymmetry in Sierra Nevada Glacier length during the Last Glacial Maximum. *J. Geophys. Res.* **111**, F02002 (2006).
23. Løken, O. H. & Hodgson, D. A. On the submarine geomorphology along the east coast of Baffin Island. *Can. J. Earth Sci.* **8**, 185–195 (1971).
24. Hughes, T. Calving bays. *Quat. Sci. Rev.* **21**, 267–282 (2002).
25. Meier, M. F. & Post, A. Fast tidewater glaciers. *J. Geophys. Res.* **92**, 9051–9058 (1987).
26. Pfeffer, W. T. A simple mechanism for irreversible tidewater glacier retreat. *J. Geophys. Res.* doi:10.1029/2006JF000590 (2007).
27. Broecker, W. S. Massive iceberg discharges as triggers for global climate change. *Nature* **372**, 421–424 (1994).
28. Oerlemans, J. An attempt to simulate historic front variations of Nigardsbreen, Norway. *Theor. Appl. Climatol.* **37**, 126–135 (1986).
29. Pfeffer, W. T. *et al*. Numerical modeling of late Glacial Laurentide advance of ice across Hudson Strait: Insights into terrestrial and marine geology, mass balance, and calving flux. *Paleoceanography* **12**, 97–110 (1997).
30. Gjessing, J. Om iserosjon, fjorddal- og dalendedannelse; on ice erosion, fiord-valley and valley-end formation. *Norsk Geografisk Tidsskrift* **15**, 243–269 (1956).

Acknowledgements

This research was partially financially supported by NSF (EAR-0644966; EAR 0549566). Support for M.A.K. came from CU postdoctoral research funds and N. Kessler. We appreciate careful reading of an early manuscript by Y. Axford, M. M. Berlin, D. Hess, M. Duhnforth, D. Ward, B. Hallet and T. Stern.

Author information

Reprints and permission information is available online at http://npg.nature.com/reprintsandpermissions. Correspondence and requests for materials should be addressed to M.A.K.